JOURNAL OF Applied Polymer SCIENCE

PP/PP-g-MAH/Layered Expanded Graphite Oxide Nanocomposites Prepared Via Masterbatch Process

Jun Bian,[1] Xiao Wei Wei,[1] Hai Lan Lin,[1] I Ta Chang,[2] Erol Sancaktar[2]

[1]Key Laboratory of Special Materials and Preparation Technologies, College of Materials Science and Engineering, Xi-hua University, Chengdu, Sichuan 610039, People's Republic of China

[2]Department of Polymer Science and Engineering, Polymer Engineering Academic Center, University of Akron, Akron, Ohio 44325-0301

Correspondence to: J. Bian (E-mail: bianjun2003@163.com)

ABSTRACT: Electrically conducting polypropylene/poly(propylene)-grafted maleic anhydride/layered expanded graphite oxide nanocomposites PP/PP-g-MAH [PPM/layered expanded graphite oxide (LEGO)] have been prepared by masterbatch-melt blending process. The effects of the filler and compounding method on the structure and properties of PPM/LEGO nanocomposites were investigated and reported. Scanning electron microscopy revealed excellent dispersion of LEGO in polymer matrix during the compounding process, as well as deformational features of fracture surfaces. X-ray diffraction and transmission electron microscopy (TEM) exhibited an exfoliated structure of LEGO in polymer. Fourier transform infrared spectra showed possible interfacial interactions between LEGO and matrix. Tensile tests indicated that LEGO had a reinforcing effect on the tensile behavior of PPM. Differential scanning calorimetric results showed that the incorporation of LEGO could increase T_c and X_c of polymer matrix, indicating that the LEGO acted as a nucleating agent for PPM. The nanocomposites prepared by masterbatch-melt blending showed higher conductivity than nanocomposites prepared by conventional direct melt blending. The enhancement of electrical conductivity may be due to more effective dispersion of LEGO sheets in the polymer matrix and strong interfacial interactions between LEGO and matrix, which reinforced the formation of conducting multiple networks. © 2012 Wiley Periodicals, Inc. J. Appl. Polym. Sci. 000: 000–000, 2012

KEYWORDS: composites; properties and characterization; synthesis and processing; thermal properties; mechanical properties

Received 11 April 2012; accepted 23 June 2012; published online
DOI: 10.1002/app.38243

INTRODUCTION

There is great interest in using graphene-based materials as fillers for polymer composites owing to the significant multifunctional property enhancements observed in these systems.[1–4] In recent studies, most graphene-based composite filler materials have been derived from graphite oxide (GO). GO can be produced by several different methods,[5] all of which generate a product that has a larger interlayer spacing than graphite along with several oxygen-based functional groups decorating the basal planes and edges of the platelets (e.g., carboxylic acids, epoxides, and alcohols)[6] in addition to the reported existence of strongly bound "oxidative debris."[7] These structural features act in tandem to facilitate the exfoliation of GO into individual graphene oxide sheets in water and certain polar organic solvents. Once dispersed in a solvent, treatment with chemical reductants such as hydrazine or sodium borohydride can afford single-layer dispersions of reduced graphene oxide with the aid of electronic or steric stabilization.[7,8] It has also been shown that GO can be exfoliated and reduced via thermal shocking[9,10] (i.e., rapid heating under inert gas) or microwave treatment[10] to create loosely stacked, "wormlike" structures with a high specific surface area.

Solvent-exfoliated graphene oxide platelets as well as thermally layered expanded GO (LEGO) particles have been widely investigated as fillers for polymer composites.[1] In particular, LEGO can be dispersed into a polymer matrix via melt mixing operations which are highly compatible with industrial practice.[11–15] In our previous works, expanded graphite (EG) was prepared by thermal shock and used in PES[16] and PA11-based[17] nanocomposites. LEGO has a similar structure to EG, which suggests that LEGO may also disperse using melt mixing and might afford property enhancements comparable to EG. However, there are also some important differences in the reported physical properties of LEGO and EG, such as different C : O ratios (i.e., a generally lower C : O ratio for LEGO compared to EG), which could possibly affect dispersion and the final composite

properties.[1] In light of these differences, we sought to investigate the property enhancements afforded by LEGO, using commonly used thermoplastics-PP and PP-g-MAH as "model" matrix polymers, using melt mixing to mix LEGO with PP/PP-g-MAH (PPM) to create well-dispersed PPM/LEGO nanocomposites without the aid of solvents. Nevertheless, since the dispersion and size distribution of LEGO in polymers are not as good as expected, especially those prepared by conventional direct melt extrusion under limited extrusion times, the aggregations in these composites may lead to poor interfacial interactions, and thus, poor mechanical properties. Interestingly, homogeneous distribution of fillers within polymer can be achieved by masterbatch filling technique. Lepoittevin et al.[18] examined polymer/layered silicate nanocomposites prepared by a masterbatch process. They showed that clay could be further exfoliated by this method and the mechanical properties of the composite were improved in comparison to those obtained by direct melt extrusion. Potschke et al.[19] studied a well-treated PC/CNT masterbatch-filled PE matrix and found that a lower percolation threshold was observed as a result of appropriate mixing conditions. Li and Chen[20] prepared HDPE composites with different amounts of EG-based masterbatches using melt blending. They also found that the mechanical and thermal properties for the nanocomposites were improved by masterbatch process, and the results depended greatly on the dispersion of EG and compatibility between the masterbatch and the matrix.

This work focuses on PPM/LEGO nanocomposites prepared by an effective processing method involving masterbatch-melt blending. Highly filled PPM/LEGO masterbatches were first prepared by melt blending, followed by further melt blending of this masterbatch with additional PP. Electrical, thermal, and mechanical properties of the PPM/LEGO nanocomposites prepared using this "two-step" method were studied extensively and discussed. Herein, we present, to our knowledge, the first report on the morphology and properties of LEGO-filled PPM nanocomposites.

EXPERIMENTAL

Materials

PP (T30S) was kindly provided by Dushanzi Fule & Chemical Co., (XingJiang, China). PP-g-MAH with a graft ratio of 0.7–0.8 wt % and a melt index of 12 g/10 min was supplied by Nan-Jing Julong Chemical, (NanJing, China). PP-g-MAH was dried under vacuum at 80°C for one night before use. Natural graphite powder [NGP, SP-2, ($C > 99\%$, $D = 5$ μm)] was purchased from Qingdao Tianhe Graphite (QingDao, China). $KMnO_4$ (C.P.), concentrated H_2SO_4 (>96%), H_2O_2 and isopropyl alcohol (IPA) were purchased from KeLong Reagent, (ChengDu, China) and used as received.

Preparation of GO and LEGO

GO used in this research was first synthesized from NGP by graphite oxidation with $KMnO_4$ in concentrated H_2SO_4 according to modified Hummer's method with the detailed procedure provided in Ref. 21. GO flakes were then rapidly exfoliated at 800°C for 30 s in a preheated muffle furnace to cause rapid exfoliation and reduction of the material. The black, fluffy powder was collected and kept free to maintain its original morphology before use.

Fabrication of Masterbatches and PPM/LEGO Nanocomposites

The weight ratio of PP to PP-g-MAH was 1 : 1, constant for all samples. The nanocomposites contained LEGO at the weight percent loadings of 0, 1.96, 3.84, 5.66, and 7.41, as prepared by combination of masterbatch and melt blending processing. In the first step of processing, all LEGO and PP-g-MAH to be used were melt-blended with 50 wt % of total PP to be used. Since LEGO has low bulk density (0.02–0.03 g/mL), some LEGO powder is easily lost during handling and particularly during the mixing step. To minimize this problem and to improve the dispersion of LEGO fillers in the composites, we applied a coating method reported in our previous works.[16,17] LEGO was first dispersed in IPA by sonication for 3 h at room temperature, PP and PP-g-MAH powder was then added to this LEGO solution and sonication was continued for 1 h. Finally, the solvent was evaporated at 80°C resulting in complete coverage of the powder particles with LEGO. Once the compounding was completed, the PPM/LEGO masterbatches were prepared by melt blending in a twin-screw extruder (TSE-30 A/500-11-40, RuiYa Polymer Processing Equipment, NanJing, China. The diameter of the screw was 30 mm and the L/D (length/diameter) ratio was 36. The extrusion temperatures from hopper to die were 180, 195, 200, 205, 210, 215, 220, 220, and 210°C. The screw speed was 100 rpm and the residence time was about 3–5 min.

The PPM/LEGO masterbatches obtained in the first step were diluted with the remaining 50 wt % of the total PP to be used in the same TSE using the same conditions as in the first step to prepare the final PPM/LEGO nanocomposties. After extrusion, all samples were chopped into pellets to prepare test specimens of 50 × 10 × 4 mm^3 dimensions using an injection molding machine (TTI-90Φ35, Donghua Machine, Guangdong, China). The temperatures of different zones were (from hopper to die): 200, 210, 220, and 230°C. The mold temperature was ambient temperature. The screw speed was 120 rpm and the injection pressure was kept at around 15 MPa.

For comparison, neat PP samples were prepared under identical extrusion and injection conditions (temperatures, screw speed, and pressure). For conventional melt blending PPM/LEGO nanocomposites containing various amounts of LEGO (0, 1.96, 3.84, 5.66, and 7.41 wt %), coating method was also used to produce a complete coverage of the PPM matrix with LEGO prior to mixing. Upon completion of coating, dried PPM/LEGO mixtures were processed via melt blending followed by injection molding to produce the final nanocomposites using the same conditions.

Characterization

Microscopy and Structure. The microscopic images of samples were collected using a scanning electron microscope (SEM) (JEOL JSM-820). The powder samples and tensile fracture surfaces of PPM/LEGO with different LEGO contents were coated with gold before SEM examination. Transmission electron microscopy (TEM) (Tecnai G^2 F20 S-TWIN) micrograph

was performed using an acceleration voltage of 100 kV. Ultrathin samples were obtained using a LEICA microtome.

X-Ray Photoelectron Spectra (XPS). XPS of samples was obtained by using an ESCALAB 250 (Thermo-VG Scientific) analyzer. The Al K_a radiation (hv = 1253.6 eV) used was monochromatized. Survey scan spectra in the 1200–0 eV binding energy range were recorded with pass energy of 20.0 eV.

X-Ray Diffraction. The test was performed on the Rigaku D/max-1200X Diffractometer (40 kV, 200 mA, Cu *K*a, λ = 0.154 nm) at ambient temperature. Scans were taken from 1.5° to 60° with a step of 0.02° at 40 kV and 30 mA. The NGP, GO and LEGO samples were in fine powder form, whereas PP, PP-g-MAH, and PPM/LEGO composites samples were from injection-molded standard tensile testing specimens.

Fourier Transform Infrared Spectroscopy. The Fourier transform infrared (FTIR) was observed at room temperature on a Nicolet 380 spectrometer (Thermo Electron Corporation, USA) with a resolution of 4 cm^{-1}. The powder specimens were dispersed into the KBr powder by mortar, and compressed to form disks. The nanocomposite samples were from injection-molded standard tensile testing specimens. They were dried at 80°C under vacuum for 6 h before analysis.

Thermogravimetric Analysis. The thermal stability of PPM/LEGO was determined using a Perkin-Elmer TGA7 Thermogravimetric Analyzer. The sample mass analyzed was typically 5–7 mg using an open platinum pan. PPM/LEGO specimens were heated from 30 to 700°C at a heating rate of 20°C/min, under a nitrogen atmosphere. The onset of degradation temperature ($T_{d,onset}$), maximum rate of degradation temperature ($T_{d,max}$) and other data were determined from the weight loss curves.

Differential Scanning Calorimetric Analysis. Differential scanning calorimetric (DSC) analysis was carried out on NETZSCH DSC-200PC under N_2 atmosphere. Samples were heated from room temperature to 250°C at a rate of 20°C/min and held at that temperature for 10 min to eliminate the heat history. The samples were then cooled to 30°C at a rate of 100°C/min. After keeping at 30°C for 5 min, samples were heated to 250°C at a rate of 20°C/min again. The crystallization (T_c) and melting (T_m) temperatures were determined from maxima of the cooling and reheating scans, respectively.

Mechanical Properties. Tensile properties were obtained using an INSTRON3365 electronic tensile tester with computer control. The rate of cross-head motion was 20 mm/min at room temperature. Five specimens of each composition were tested, and the average values were reported.

Electrical Conductivity. The conductivity (σ) of nanocomposites was measured using electrochemical workstation (Solartron 1255B) at room temperature when σ was less than 10^{-3} S/cm. When σ of the specimen was greater than 10^{-3} S/cm, it was measured using an SDY-4 four-probe instrument (Guangzhou, China). The detailed procedures and calculation methods have been reported in our previous works.[16,17]

RESULTS AND DISCUSSION

Morphology of Fillers

The as-received NGP is composed of thin graphite flakes. As shown in Figure 1(a), the layered structure of graphite flakes are regular and the interlayer distance is small [approximately 0.335 nm according to X-ray diffraction (XRD)]. GO consists of parallel platelets stacked in a periodic fashion and demonstrates a flaky surface [Figure 1(b)]. When GO is exposed to thermal shock, graphite layers exfoliate to form a structure often referred to as LEGO. LEGO has a fluffy, lightly stacked structure of wrinkled platelets as shown in Figure 1(c–e). This structure forms an interconnected network when incorporated into a polymer matrix such as PPM. XPS measurements indicate that as-prepared GO has a C : O ratio of 1.4 : 1, while LEGO is found to have a C : O ratio of 3.2 : 1, indicating the presence of oxygen-based functional groups on the LEGO platelets, although in much lower concentration than GO [Figure 1(g). Upon dispersion of LEGO into PPM, the nanocomposites become black in color and become completely opaque, as shown in Figure 1(f).

The diffractograms of NGP, GO, and LEGO are shown in Figure 2. The original NGP shows a (002) diffraction peak at 2θ = 26.6°, which is corresponding to the *d*-spacing of 0.335 nm. Upon oxidation, the diffractogram of GO consists of peaks within the 2θ range 10–12° and 25–26°. The peaks within these ranges correspond to the diffraction of (001) and (002) planes representing the GO and graphite peak, respectively. In the case of LEGO, the (002) peaks are observed in the same 2θ range when GO was exfoliated at high temperatures to form LEGO. The shifting in the (002) peaks to lower 2θ indicates separation of graphite layers. In addition, the (001) peak is absent in either diffractograms, suggesting that graphite platelets have completely been exfoliated. As LEGO is largely exfoliated (relative to GO) before mixing into the PPM matrix, it is expected that the nanocomposites of LEGO would exhibit an exfoliated morphology. This expectation will be confirmed by subsequent XRD, SEM, and TEM characterizations.

XRD Analysis of Nanocomposites

The diffractograms of PP, PP-g-MAH, unfilled PPM, as well as PPM/LEGO, are shown in Figure 3. The data obtained from XRD are listed in Table I. PPM shows similar XRD diffractograms to those of PP and PP-g-MAH. The unfilled PP or PPM provide three prominent characteristic peaks corresponding to the diffraction (110) (Pk1), (040) (Pk2), and (130) (Pk3) planes at 2θ = 13.74, 16.56, and 18.14° which correspond to the monoclinic (α) crystalline phase of PP or PPM.[22–24] It should be noted that, a β peak at 2θ around16° is not visible on the shoulder of Pk2, which is different from Cerezo et al.[25] report. In Figure 3, the diffractograms of PPM/LEGO showed (α) peaks within the 2θ range of 10–30° and a (002) peak (Pk4) at 2θ = 26.32°. The β peak is still not visible for all of PPM/LEGO nanocomposites. The diffractograms of PPM/LEGO demonstrate shifts to higher 2θ for Pk1 and Pk2. These shifts indicate tighter packing in the crystal unit cell in directions perpendicular to the chain direction.[25]

Applied Polymer SCIENCE

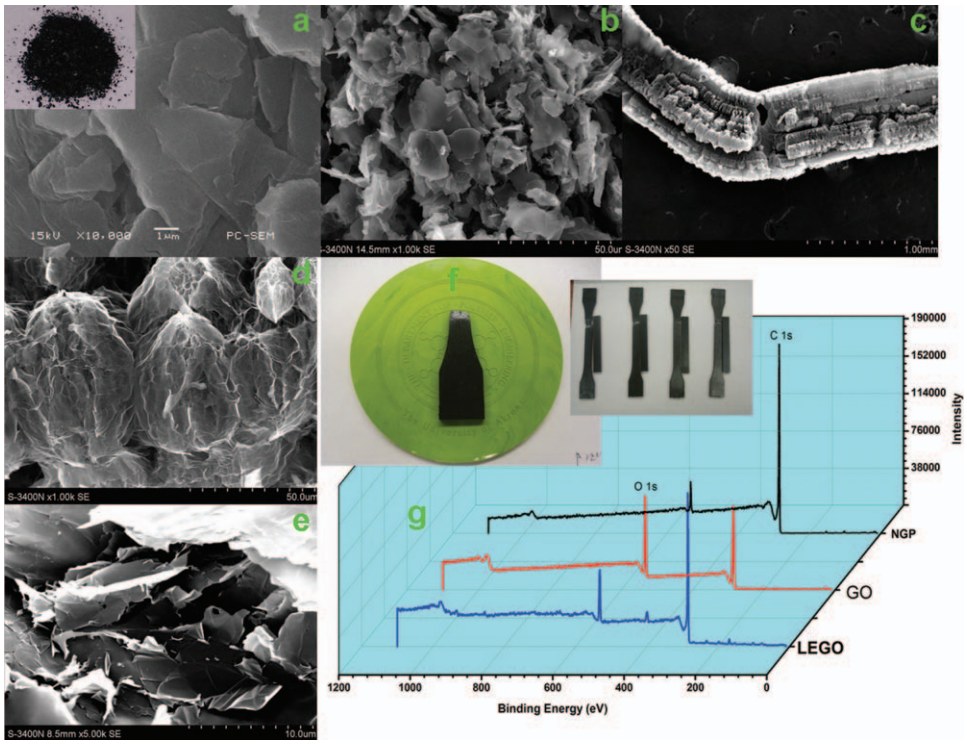

Figure 1. (a) SEM and digital image (inset) of NGP. (b) SEM image of GO. (c) SEM image of LEGO. (d–e) Higher magnification SEM images of LEGO. (f) Injection-molded samples showing the loss of optical clarity in PPM/LEGO as a function of loading. (g) XPS spectra of NGP, GO, and LEGO. [Color figure can be viewed in the online issue, which is available at wileyonlinelibrary.com].

Figure 3 shows the changes of the relative intensities of Pk1 and Pk2 in the diffractogram of PPM/LEGO. The variation of the intensity of Pk2 in comparison to Pk1 is determined from XRD and shown in Table I. The intensity ratio of Pk2/Pk1 is considerably higher for PPM/LEGO nanocomposites than for the unfilled PPM. Zipper et al.[26] have reported similar findings. They found that the high value for Pk2/Pk1 in the presence of graphite could be attributed to the strong preferential orientation parallel to the surface of PPM/LEGO. Furthermore, the high value of Pk2/Pk1 suggests high order of crystallinity. Therefore, it is assumed that there was a higher concentration of graphite particles serving as nucleating sites present in PPM/LEGO. The nucleating effect of LEGO in PPM matrix will be further investigated with the crystallization and melting behavior of PPM/LEGO using DSC, and discussed below.

The d spacings for 3.84 and 7.41 wt % of LEGO in PPM calculated from the Bragg equation ($d = \lambda/2 \sin \theta$, where λ is the wavelength of incident radiation and θ is the diffraction angle) are shown in Table I. The d spacing of the graphite layers increases when LEGO is incorporated in PPM. This indicates that graphite layers in the PPM/LEGO are disordered and the mixing methods used are able to affect the order in the structure or exfoliate the graphite layers within the PPM matrix. The crystalline thickness perpendicular to the reflection plane ($L_{(hkl)}$) can be determined from the Scherrer equation ($L_{hkl} = K\lambda/\beta_0 \cos \theta$, where θ is the Bragg angle, λ is the X-ray wavelength (nm); β_0 is the width of the diffraction beam (radians); K is a shape factor related to the structure of crystalline thickness as well as β_0 and $L_{(hkl)}$. Note that when β_0 is defined as half-height width of diffraction peaks, we have $K = 0.9$[25]). In this case, the graphite peak, $L_{(002)}$, is of interest and is used to determine the crystalline thickness of LEGO in PPM matrix. The results are summarized in Table I and show that the crystalline thickness of LEGO in PPM/LEGO is higher in comparison to that of homogeneous LEGO, but still in the nanometer scale. The increase in the $L_{(002)}$ suggests that PP-g-MAH intercalation occurs within the graphite layers.

To confirm the exfoliated morphology of LEGO revealed by XRD, further investigation of structural characteristics of the

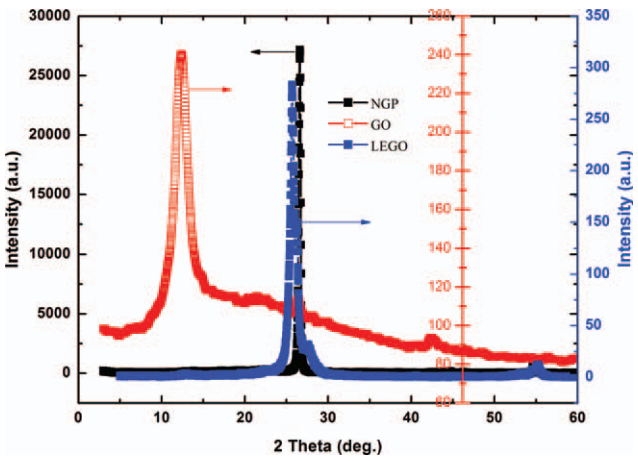

Figure 2. XRD patterns of NGP, GO, and LEGO. [Color figure can be viewed in the online issue, which is available at wileyonlinelibrary.com].

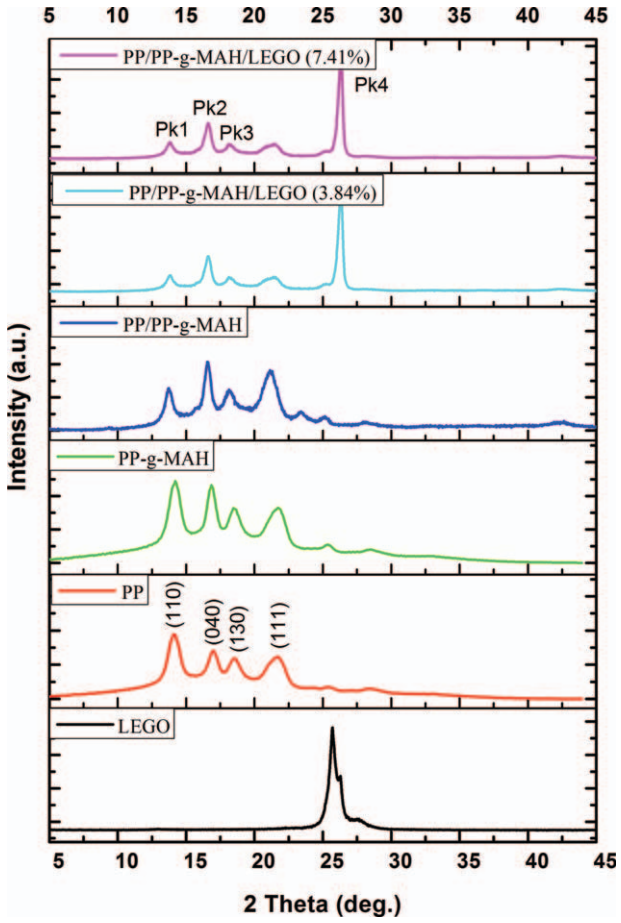

Figure 3. XRD patterns of LEGO, neat PP, PP-g-MAH, PPM, and PPM/LEGO nanocomposites. [Color figure can be viewed in the online issue, which is available at wileyonlinelibrary.com].

nanocomposites are carried out using TEM. PPM/LEGO (3.84 wt %) nanocomposite is selected and the TEM micrograph is shown in Figure 4. The black lines and white domains are identified as LEGO sheets and polymer matrix, respectively. It can be observed that the LEGO sheets are well dispersed in PPM matrix with the thickness of about 30–50 nm and are parallel to each other, indicating efficient formation of PPM/LEGO nanocomposites by melt blending. Moreover, many of the platelets appear to be in contact in the images, suggesting that the LEGO particles have formed a percolating network at this loading, consistent with our electrical measurements.

Infrared Spectroscopy of Fillers and Nanocomposites

The interaction of polymer composites can be identified by FTIR spectra. It is known that, if two polymers are compatible, a distinct interaction (hydrogen-bonding or dipolar interaction) can exist between the chains of the two polymers, causing the infrared spectra of the composite to change (e.g., band shifts and broadening).[27] Consequently, FTIR can identify segmental interactions and provide information about the phase behavior of polymer composites. Figure 5 shows the FTIR spectra of fillers and NGP, GO, LEGO fillers, PP, PP-g-MAH, PPM polymers, and PPM/LEGO nanocomposites. As shown in Figure 5, almost no absorbance peaks are detected for NGP. GO shows sharp peaks at 3431, 2950–2860, 1714, 1625, and 1045 cm^{-1}. The broad and strong absorption band centered at around 3431 cm^{-1} is attributed to the —OH stretching mode in carboxylic acid group and also inferred to the presence of hydroxyl (—OH) group on the GO surface. The results indicate that carboxylic acid group is attached to the surface of GO.[28] The peaks at 2950 and 2860 cm^{-1} are correspond to the stretching vibration of $—CH_3$, $>CH_2$, and >CH— groups. The absorbance peak at 1720 cm^{-1} is assigned to the stretching vibrations of acid carbonyl (>C=O) group of the carboxylic acid groups present on the GO surface. The peak 1625 cm^{-1} is assigned to the stretching vibration of C=C bond in aromatic ring of graphite. The peak at 1045 cm^{-1} is referred to the vibration of C—O bond in primary alcohol and the C—O stretching mode of the characteristic of ether linkage (C—O—C) present on the GO surface.[28,29] For LEGO, although the intensity of most absorbance peaks are decreased, the absorbance peaks at 3510, 2943, 1719, 1651, and 1184 cm^{-1} can still be distinguished to represent the same functional groups same as on GO surfaces. We believe that these surface characteristics are helpful in improving the interfacial interactions between LEGO and polymeric matrices, thus resulting in improvement of mechanical properties. For PP, characteristic peaks are clearly seen in the range of 2800–2900 cm^{-1} and range of 1400–1300 cm^{-1}, representing the asymmetric and symmetric vibrations of $—CH_2—$.

Table I. XRD Results of Samples

Samples	2θ angle (°) and ascription						
	Pk1 (110)	Pk2 (040)	Pk3 (130)	Pk4 G (110)[a]	Pk2/Pk1	*d* spacing,nm[b]	$L_{(002)}$, nm[c]
LEGO	-	-	-	25.72	-	0.330	17.7
PP	14.06	16.96	18.54	-	0.75	-	-
PP-g-MAH	14.21	16.91	18.58	-	0.96	-	-
PP/PP-g-MAH	13.74	16.56	18.14	-	1.38	-	-
PP/PP-g-MAH/LEGO(3.84%)	13.86	16.60	18.14	26.32	2.04	0.333	29.4
PP/PP-g-MAH/LEGO(7.41%)	13.86	16.60	18.12	26.32	2.10	0.338	33.6
Shift[d]	+0.12	+0.04	-	+0.60	-	-	-

Including 2θ, intensity ratio of a peaks 040/110 (Pk2/Pk1), and crystalline thickness of LEGO in PP/PP-g-MAH/LEGO composites.
[a]"G" denotes graphite, [b]Calculated from Bragg equation, [c]Calculated from Scherrer equation, [d]"+"denotes shifting to higher angle.

Applied Polymer SCIENCE

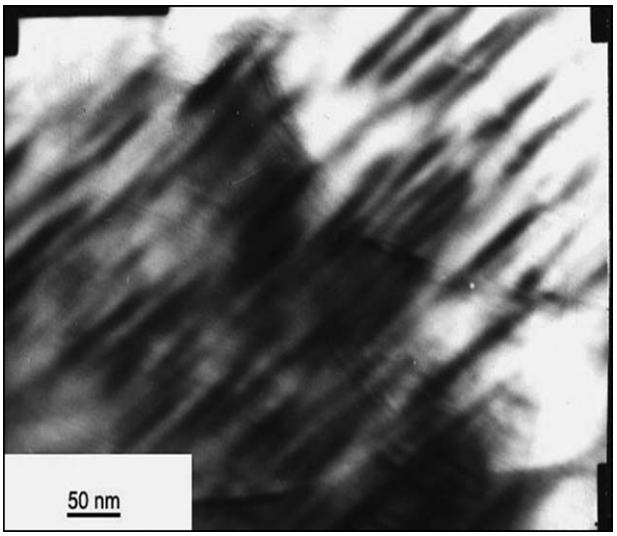

Figure 4. TEM micrograph of PPM/LEGO (3.84 wt %) nanocomposite.

For PP-g-MAH, the intensities of absorbance peaks in the range 2800–2900 cm^{-1} are decreased, but characteristic peaks of MAH are clearly seen at about 1784 (—C=O), 1518 and 800–1200 cm^{-1}.The absorbance spectrum of PPM is similar to that of simple stack of PP and PP-g-MAH, indicating the absence of specific interactions between them. Shifts in absorbance band and changes in intensity are observed after blending with LEGO. Especially the absorbance at about 1780 and 800–1200 cm^{-1} for PPM/LEGO (7.41 wt %) nanocomposites decreased, which provides the possible physical interaction due to the hydrogen bond between the —COOH and —OH groups of the LEGO and >C—O group of the PP-g-MAH.

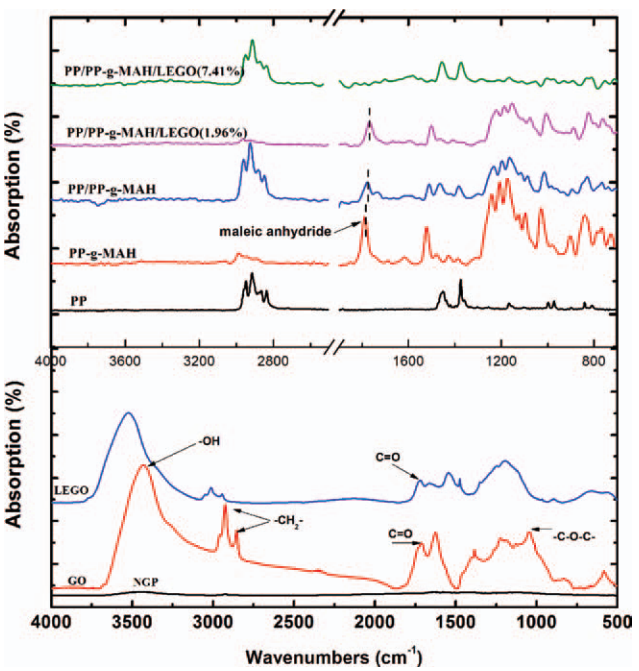

Figure 5. FTIR spectra of NGP, GO, LEGO, PP, PP-g-MAH, PPM, and PPM/LEGO nanocomposites. [Color figure can be viewed in the online issue, which is available at wileyonlinelibrary.com].

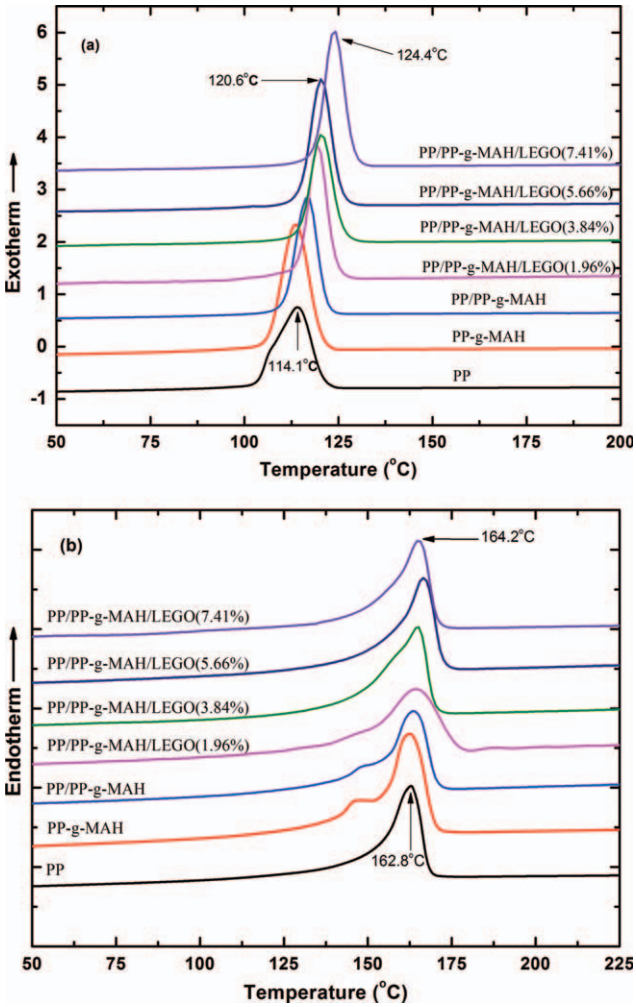

Figure 6. DSC curves of samples. (a) Crystallization curves and (b) melting curves of neat PP, PP-g-MAH, PPM, and PPM/LEGO nanocomposites with different LEGO contents. [Color figure can be viewed in the online issue, which is available at wileyonlinelibrary.com].

Crystallization and Melting Behaviors of Nanocomposites

The DSC thermograms of PP, PP-g-MAH, and PPM/LEGO are shown in Figure 6. The characteristic peak due to the monoclinic (α) crystalline phase of PPM in both the crystallization (T_c) exotherms and melting (T_m) endotherms can be observed in Figure 6, thus confirming the XRD findings. The T_c and T_m values for PP, PP-g-MAH, and PPM/LEGO with different LEGO loadings are listed in Table II. The neat PP shows a T_c of 114.1°C and a T_m of 162.8°C. For neat PP-g-MAH, a T_c of 113.6°C and a T_m of 162.9°C can be observed. Unfilled PPM has a T_c of 116.3°C and a T_m of 163.2°C. In the presence of LEGO, the T_c of PPM shifts to higher temperatures as LEGO content increases. A similar trend in T_m is observed for the PPM/LEGO composites (only modest increases in T_m when LEGO is equal to or higher than 5.66 wt %). The enhancement in T_c and T_m of PPM/LEGO is attributed to the mixing

Table II. DSC Results of Samples, Including Crystallization, Melting Temperatures and Crystallinity of PP/PP-g-MAH/LEGO Nanocomposites

Samples	T_c (°C)	T_m (°C)	X_c
PP	114.1	162.8	0.49
PP-g-MAH	113.6	162.9	0.47
PP/PP-g-MAH	116.3	163.2	0.48
PP/PP-g-MAH/LEGO(1.96%)	119.2	165.2	0.50
PP/PP-g-MAH/LEGO(3.84%)	120.3	166.5	0.51
PP/PP-g-MAH/LEGO(5.66%)	120.6	164.7	0.53
PP/PP-g-MAH/LEGO(7.41%)	124.4	164.2	0.55

method. PPM/LEGO obtained from masterbatch disrupts the graphite layers, separating them and thus providing more surfaces for nucleation. Increases in T_c and T_m have also been reported for PP-clay[30] and PPS-graphite[31] composites. These results show that LEGO behaves as a nucleating agent. Introduction of LEGO provides more nucleating sites as a result of its large surface area.

The crystallinity (X_c) of the materials is calculated and shown in Table II. A marginal increase in the X_c of PPM is observed due to the presence LEGO. Overall, the DSC analysis clearly shows that incorporating LEGO in PPM results in an increase in T_c, T_m, and X_c. These observations show that LEGO is an efficient nucleating agent for PPM. Presumably, the increase in the T_c, T_m, and X_c of the PPM relates to the surface area of the included LEGO.

Thermal Degradation of PPM/LEGO Nanocomposites

Graphene fillers have been widely reported to improve the thermal stability of polymer composites relative to the host polymer.[1–3] Thermal degradation studies of the composites were performed using thermogravimetric analysis (TGA) and the results are presented in Figure 7. For comparison purpose, the thermal stability of pure PP, PP-g-MAH, and PPM are also shown. The weight loss curves (TGA curve) of filled and unfilled PPM show that degradation occurs in one-step from 400 to 550°C. This process is attributed to main chain scission, predominately with the evolution of carbon and oxygen functional groups, resulting in the observed weight loss. At temperatures beyond 550°C, no residue remains. The TGA curves of all PPM/LEGO materials studied show that degradation occurred in a similar manner as with pure PPM. However, the initial degradation begins at temperatures as low as 365.6°C. This probably related to the loss of low-molecular weight products such as acids or intercalants retained in the graphite layers. The obvious trend observed is that the thermal stability of composites with different LEGO loadings is better than PP-g-MAH but somewhat poorer than PP. The high T_d observed for PPM/LEGO is considered to be related to the tortuous path of degradation products, which is strongly related to the distribution of graphite particles in the PP-g-MAH matrix and hence dependent on the mixing method. In addition, it is observed that a stable char is formed from some of the PPM/LEGO materials at temperatures beyond 600°C, as listed in Table III. The char layer containing LEGO is believed to offer protection to the underlying polymer from degradation by acting as a physical barrier that limits the heat and mass transfer between the gas and condensed phases and thereby delaying degradation of PPM. The increase in char content has been reported by Qu and Xie,[32] who claimed positive evidence that LEGO can promote the formation of carbonaceous materials in the condensed phase.

Tensile properties

To investigate the effects of processing methods and LEGO loading on the mechanical properties of the composites, injection-molded tensile specimens were tested. A comparison of mechanical properties is provided in Figure 8. The addition of LEGO significantly increases the Young's modulus [YM, see Figure 8(a)] as well as the yield strength [YS, Figure 8(b)] and break strength [BS, Figure 8(c)], but reduces the elongation at break [EB, Figure 8(d)]. Figure 8(a) shows that pure PP and PP-g-MAH (gPP) have relatively low YM, but YM increases with increasing LEGO loading within a weight fraction of 7.41%, particularly when the weight fraction is more than 1.96%. The highest YM was 2.23 GPa for the nanocomposite with 7.41 wt % LEGO. In addition to enhancing the YM, of

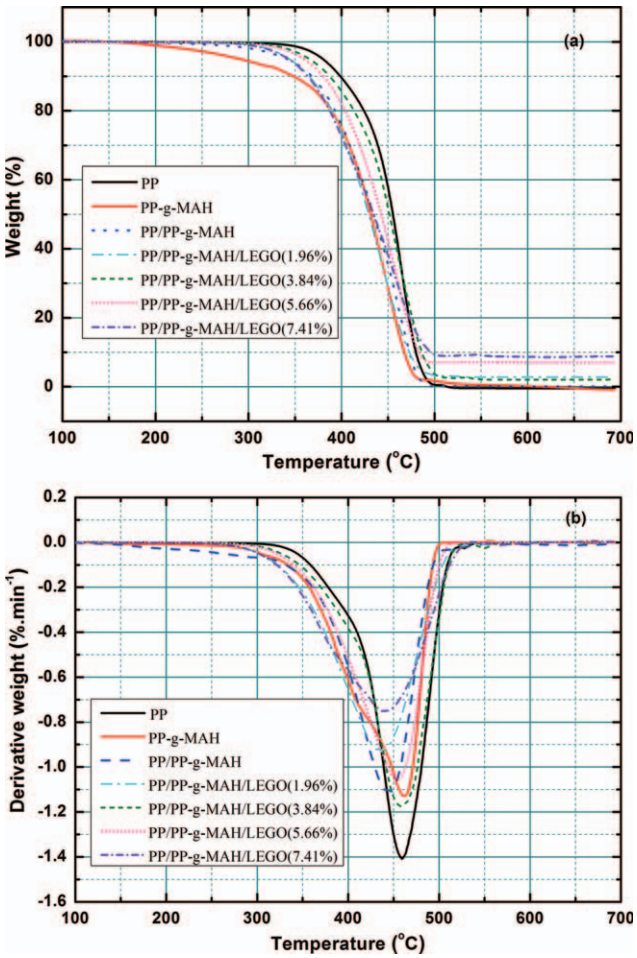

Figure 7. TG (a) and DTG (b) curve of neat PPM and PPM/LEGO nanocomposites with different LEGO contents. [Color figure can be viewed in the online issue, which is available at wileyonlinelibrary.com].

Table III. Degradation Temperatures and Char Content of PP/PP-g-MAH/LEGO Nanocomposites

Samples	$T_{d,onse}$ (°C)	$T_{d,max}$ (°C)	$T_{-5\%}$ (°C)	$T_{d,end}$ (°C)	Char (%)
PP	428.3	467.3	380.6	489.5	0
PP-g-MAH	390.7	448.3	288.7	491.7	0
PP/PP-g-MAH	372.4	461.0	341.0	481.2	0
PP/PP-g-MAH/LEGO (1.96%)	391.5	445.3	346.8	471.8	2.5
PP/PP-g-MAH/LEGO (3.84%)	377.2	464.5	369.4	478.8	2.1
PP/PP-g-MAH/LEGO (5.66%)	365.6	459.2	360.7	480.1	6.9
PP/PP-g-MAH/LEGO (7.41%)	378.1	458.6	346.9	480.7	8.7

particular interest are the increases in the YS and BS of the nanocomposites. For a polymer material, as the YS is reached, the mechanical behavior deviates from the linear elastic regime and begins to acquire plastic deformation. Therefore, lower YS means poorer deformation resistance. As shown in Figure 8(b), the YS of the composites with 7.41 wt % LEGO increases to 42.4 MPa from 29.2 MPa for the gPP, about 1.5 times of increase. The enhancements in YM and YS are attributed to the good dispersion of LEGO sheets and strong interfacial adhesion between the LEGO sheets and the matrix, which can transfer load effectively from the matrix to the LEGO sheets. Higher loads are carried by LEGO sheets at given macro-scale strains with an increase in the loading of LEGO sheets. LEGO sheets have a large number of polar groups on the graphene backbone, which can form many hydrogen bonds with PP-g-MAH chains, resulting in strong interfacial adhesion.

The addition of LEGO to PPM matrix also induces an increase in the BS and toughness (indicated by the area under the tensile stress–strain curves). The BS increases with increasing LEGO loading within a mass fraction of 7.41 wt %, in particular, the sharp increase in BS appears when the weight fraction is more than 3.84%. The highest BS is 44.8 MPa for the nanocomposite with 7.41 wt % of LEGO prepared by masterbatch method. This BS is 2.4 times higher than that for the PPM matrix (18.5 MPa). Compared with pure PP, gPP, and PPM, the toughness [Figure 8(e)] of the nanocomposite shows a remarkable enhancement by incorporating LEGO, while the EB [Figure 8(d)] is significantly decreased to 184% from 251% for pure PP, indicating that the composites are still highly ductile. Such superior mechanical properties can certainly be attributed to the strong interfacial adhesion and good compatibility between the LEGO sheets and PPM matrix, resulting in effective load transfer from the matrix to LEGO sheets. Further analysis reveals that PPM has low YM, YS, and BS compared with PPM/LEGO nanocomposites, demonstrating that LEGO delivered a significant improvement in mechanical properties of MPP matrix (Figure 8).

For the two types of composites processed using two different methods, better tensile properties are obtained using the masterbatch methods in comparison to the conventional routes. Thus, the advantages and uniqueness of using the LEGO as reinforcing nanofillers and using the masterbatch method to make polymer nanocomposites are obvious. The possible toughening mechanism(s) will be discussed below based on SEM observations.

Morphology and Reinforcement Mechanisms

To reveal the possible reinforcing mechanism(s), the tensile failure surfaces of PPM/LEGO composites were investigated by SEM. Figure 9 shows a typical overview on the fracture surfaces of the composites with different LEGO contents. Obviously, brittle fracture happens in PPM/LEGO masterbatch filling

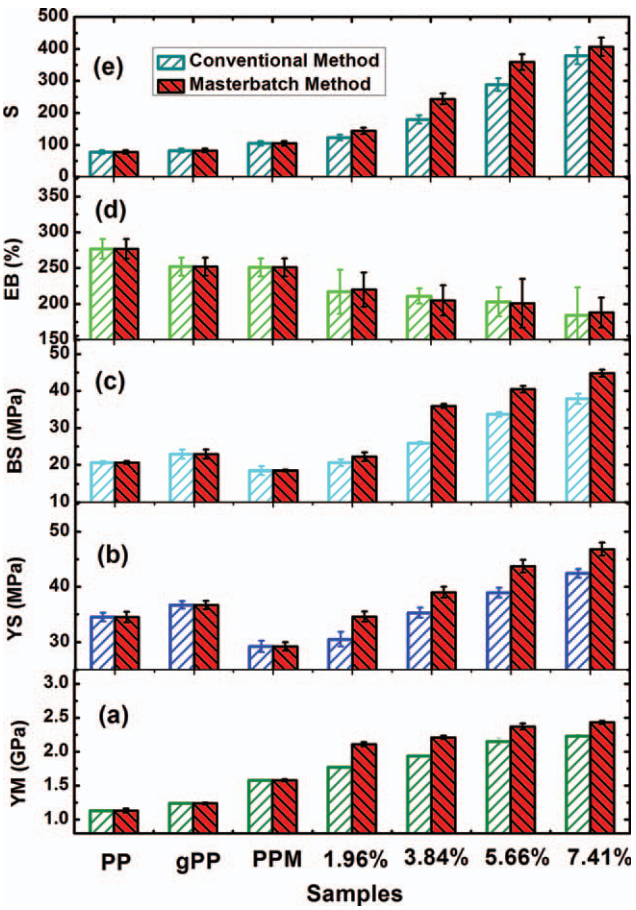

Figure 8. Mechanical properties of the nanocomposites as a function of LEGO content: (a) YM; (b) YS; (c) BS; (d) EB; (e) Toughness (S, indicating by the area under the tensile stress-strain curves). [Color figure can be viewed in the online issue, which is available at wileyonlinelibrary.com].

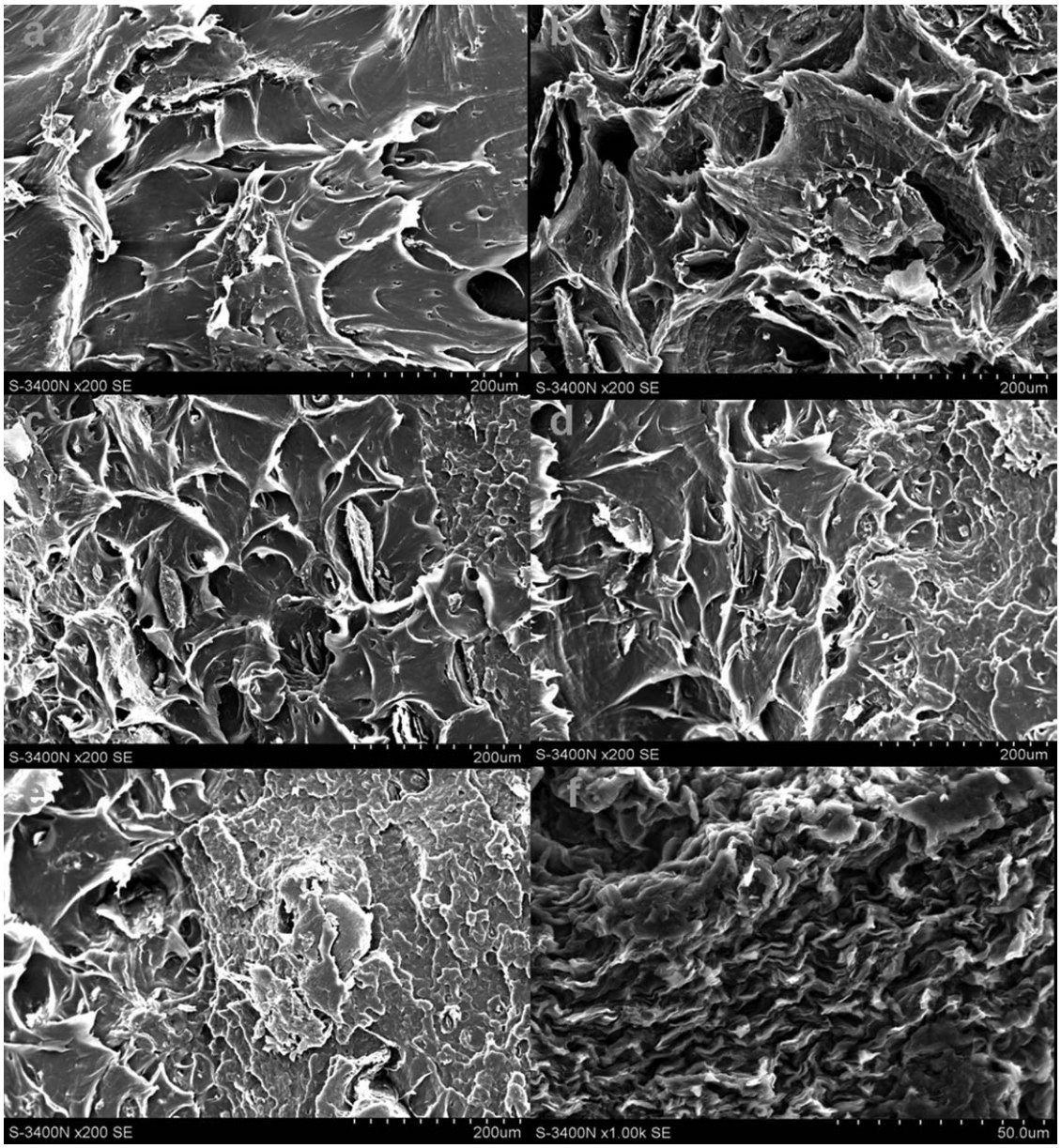

Figure 9. SEM micrographs of PPM/LEGO nanocomposites with different LEGO contents (wt %). (a) 0, (b) 1.96, (c) 3.84, (d) 5.66, (e) 7.41, and (f) low magnification of (e).

composites [Figure 9(b–f)] compared to un-filled PPM composites [Figure 9(a)], confirming the excellent dispersion obtained by masterbatch two-step method. The brittle nature is the main reason for the decrease in EB. Figure 9(b–f) shows the efficient dispersion of fillers within PPM/LEGO. Clearly, most LEGO are separated into individual layers by shear force from melt-blending and the masterbatch process improves this separation. Such even dispersion in the matrix is of great importance in making LEGO reinforced polymer composites with excellent mechanical properties. The precoating and masterbatch process are found to both reduce particle size and cause random scattering of the LEGO. In summary, our results confirmed the advantage of masterbatch process in enhancement of both LEGO dispersion and mechanical properties in the melt extrusion production.

To reveal the possible interaction between the fillers and the polymer matrix and interfacial morphology, low magnification of SEM images of PPM/LEGO masterbatches containing 3.84 and 7.41 wt % were obtained. Close inspection indicates that, upon failure, most of the LEGO are broken apart and in layered and deformed appearance on the failure surfaces, as shown in Figure 10(a,b). This interesting and typical breakage phenomenon of LEGO upon tensile stretching indicates a strong interfacial adhesion between the LEGO and the PPM matrix and a sufficient load transfer from the polymer to the LEGO.

Based on the mechanical tests and morphological observations, we can draw the conclusion that LEGO has an excellent reinforcing effect on the tensile behavior of PPM. This is thought

to be due to the H-bonding of polar groups between the PP-g-MAH and the LEGO. At the same time, the tangled structure existing in the PP matrix and PP-g-MAH chains may also contribute to the interactions between the polymer and fillers. It is thus believed that the strong interfacial adhesion observed above is responsible for the significant improvement of mechanical properties shown in Figure 8.

Electrical Conductivity

The effects of LEGO content on the electrical conductivity of PPM/LEGO composites prepared by different processes are shown in Figure 11. The conductivity of PPM is about 10^{-19} S/cm, revealing that PPM is an insulator. A rapid increase in electrical conductivity takes place when the filler content exceeds 2 wt %, indicating that the introduction of LEGO significantly improves the conductivity of PPM/LEGO with a sharp transition from an electrical insulator to an electrical semiconductor. Only 3.84 wt % of LEGO is needed to get high electrical conductivity (10^{-6} S/cm) using the masterbatch-melt blending process, but higher LEGO content (5.66 wt %) is needed to reach the same electrical conductivity when using the conventional process. In other words, lower LEGO content was required to reach the percolation threshold[1,2] when using the masterbatch-melt blending process. The notable improvement of electrical conductivity of composites results from the formation of conductive network of LEGO within the PPM matrix. As discussed in "Morphology and reinforcement mechanisms" Section, the improvement in conductivity can be attributed to the fact that during masterbatch-melt blending, the polymer molecules can intercalate the pores and galleries of LEGO more sufficiently. The ensuing physical absorption of LEGO pores, and the polar interactions between the MAH groups of PP-g-MAH and the —OH and —COOH groups on the LEGO sheets lead to the establishment of a well exfoliated but firmly contacting conductive LEGO structure. Furthermore, we believe that polymer chains can well penetrate into the pores of LEGO easily ascribed to the low viscosity of polymer under processing conditions used, leading to the destruction of closely packed LEGO morphology. Similar to ultrasonic exfoliation in alcohol bath, we can consider this process as an effective exfoliation phenomenon. Both need energy to rip the tangled LEGO structure. The more energy is used, the more exfoliated nanosheets are obtained. The energy is embodied in the processing temperature and treating time in addition to what is supplied by the mixing apparatus. In this work, precoating, supersonic treatment, and masterbatch process (dilution effect) lead to efficient filler exfoliation resulting in high efficiency in network formation. Moreover, as the intercalation process proceeds, the graphite sheets are further delaminated and exfoliated allowing more polymer molecules to intercalate and enlarge the space between them.

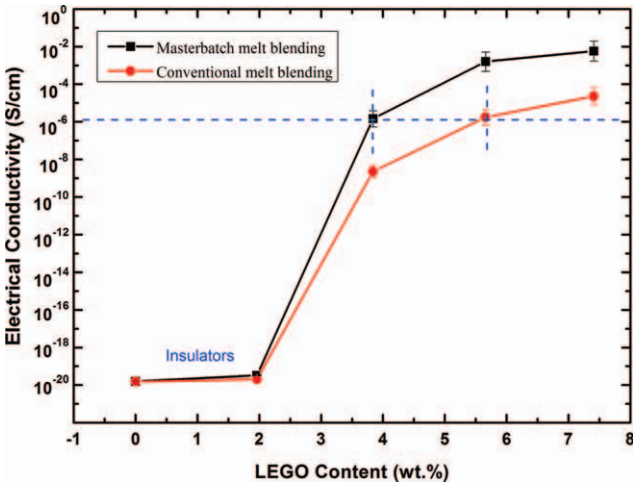

Figure 11. Electrical conductivity versus volume fraction of EG for PPM/LEGO nanocomposites prepared by two methods: masterbatch-melt blending (■) and conventional melt blending (●). [Color figure can be viewed in the online issue, which is available at wileyonlinelibrary.com].

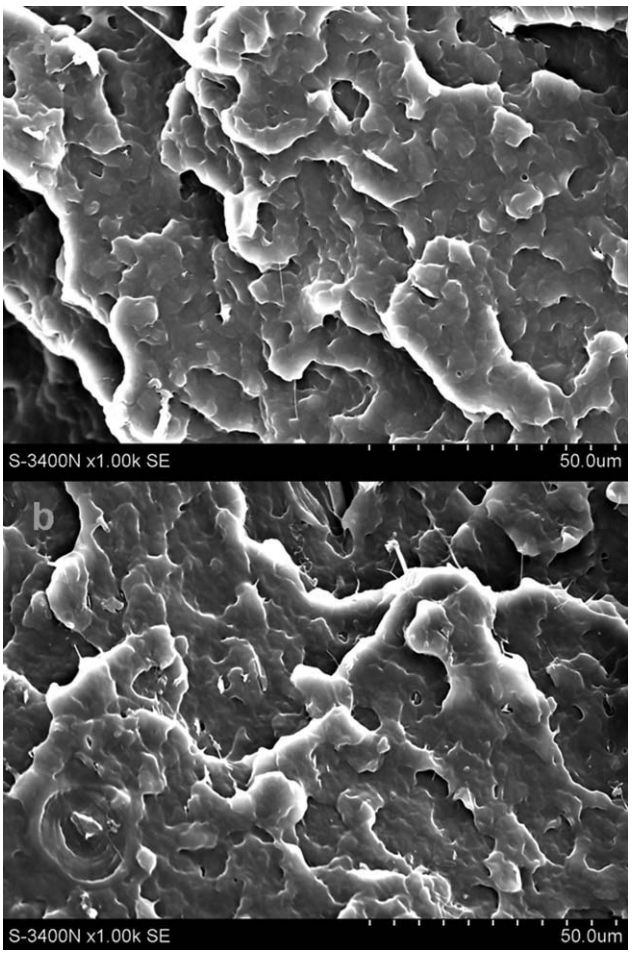

Figure 10. SEM micrographs of PPM/LEGO masterbatches with different LEGO contents (wt %). (a) 3.84, (b) 7.41.

CONCLUSIONS

LEGO-reinforced PPM nanocomposites with excellent properties have been successfully prepared by masterbatch-melt blending process. Systematic studies using different tests show that incorporation of a small amount of LEGO into PPM matrix can improve the properties of the matrix. Mechanical tests show

that incorporation of LEGO can significantly improve the strength of the matrix. Microscopic observations (SEM, TEM, and XRD) and surface characterization (FTIR) indicate uniform dispersion and exfoliated morphology of LEGO throughout matrix, as well as a strong interfacial adhesion between LEGO and the matrix leading to remarkable enhancements in overall mechanical properties. The crystallization process of PPM/LEGO in the nanocomposites is accelerated and the crystallinity increases when compared with neat PPM. Electrical conductivity of the nanocomposites increases consistently with increasing filler weight fraction. In addition, PPM/LEGO nanocomposites prepared by the masterbatch melt blending process result in higher conductivity in comparison to those prepared by the direct melt blending process.

The dispersion of LEGO into PPM via masterbatch melt mixing results in multifunctional property improvements *versus* neat PPM. However, only modest increases in thermal stability were observed in this study. But, despite this shortcoming, this study shows that LEGO can be easily dispersed into a suitable polymer matrix via masterbatch melt blending process. Given the facile synthesis of LEGO, the approach described here may provide a highly attractive route to graphene-based polymer composites.

ACKNOWLEDGMENTS

The authors thank the Chunhui Cooperation Project of the Ministry of Education (Grant No. Z2010097), Sichuan Province Youth Science Grant Program (Grant No. 11ZB005), and Xihua University Talent Fund Program (Grant No. Z0910109) for the financial supports of this work. Special thanks are also due to the Key Laboratory of Special Materials and Preparation Technologies of Xihua University and Polymer Engineering Academic Center in the University of Akron for the structural characterizations.

REFERENCES

1. Stankovich, S.; Dikin, D. A.; Dommett, G. H. B.; Kohlhaas, K. M.; Zimney, E. J.; Stach, E. A.; Piner, R. D.; Nguyen, S. T.; Ruoff, R. S. *Nature* **2006,** *442*, 282.
2. Kuilla, T.; Bhadra, S.; Yao, D. H.; Kim, N. H.; Bose, S.; Lee, J. H. *Prog. Polym. Sci.* **2010,** *35*, 1350.
3. Sengupta, R.; Bhattacharya, M.; Bandyopadhyay, S.; Bhowmick, A. K. *Prog. Polym. Sci.* **2011,** *36*, 638.
4. Potts, J. R.; Dreyer, D. R.; Bielawski, C. W.; Ruoff, R. S. *Polymer.***2011,** *52*, 5.
5. Dreyer, D. R.; Park, S.; Bielawski, C. W.; Ruoff, R. S. *Chem. Soc. Rev.* **2010,** *39*, 228.
6. Park, S.; Ruoff, R. S. *Nature. Nanotechnol.* **2009,** *4*, 217.
7. Rourke, J. P.; Pandey, P. A.; Moore, J. J.; Bates, M.; Kinloch, I. A.; Young, R. J.; Wilson, N. R. *Angew. Chem. 2011, 123*, 3231.
8. Stankovich, S.; Piner, R. D.; Chen, X.; Wu, N.; Nguyen, S. B. T.; Ruoff, R. S. *J. Mater. Chem.* **2006,** *16*, 155.
9. Ruess, V. G.; Vogt, F. *Monatsh. Chem.* **1948,** *78*, 222.
10. Schniepp, H. C.; Li, J. L.; McAllister, M. J.; Sai, H.; Herrera-Alonso, M.; Adamson, D. H.; Prud'homme, R. K.; Car, R.; Saville, D. A.; Aksay, I. A. *J. Phys. Chem. B.* **2006,** *110*, 8535.
11. Zhu, Y. W.; Murali, S.; Stoller, M. D.; Velamakanni, A.; Piner, R. D.; Ruoff, R. S. *Carbon* **2010,** *48*, 2118.
12. Yoonessi, M.; Gaier, J. R. *ACS. Nano.* **2010,** *4, 7211.*
13. Kim, H.; Macosko, C. W. *Polymer 2009, 50*, 3797.
14. Kim, H.; Miura, Y.; Macosko, C. W. *Chem. Mater. 2010, 22*, 3441.
15. Zhang, H. B.; Zheng, W. G.; Yan, Q.; Yang, Y.; Wang, J. W.; Lu, Z. H.; Ji, G. Y.; Yu, Z. Z. *Polymer* **2010,** *51*, 1191.
16. Bian, J.; Wei, X. W.; Lin, H. L.; Wang, L.; Guan Z. P. *J. Appl. Polym. Sci.,* **2012,** *12*, 3247.
17. Bian, J.; Yang, S.; Guan, Z. P. *J. XiHua Univ. (Natural Science Edition)* **2011,** *20*, 48.
18. Lepoittevin, B.; Pantoustier, N.; Devalckenaere, M.; Alexandre, M.; Calberg, C.; Jerome, R. *Polymer* **2003,** *44*, 2033.
19. Potschke, P.; Bhattacharyya, A. R.; Janke, A. *Carbon* **2004,** *42*, 965.
20. Li, Y. C.; Chen, G. H. *Polym. Eng. Sci.* **2007,** *47*, 882.
21. Bian, J.; Xiao, M.; Wang, S. J.; Wang, X. J.; Lu, Y. X.; Meng, Y. Z. *Chem. Eng. J.* **2009,** *147*, 287.
22. Saujanya, C.; Radhakrishnan, S. *Polymer* **2001,** *42*, 6723.
23. Ellis, T. S.; D'Angelo, J. S. *J. Appl. Polym. Sci.* **2003,** *90*, 1639.
24. Gopakumar, T. G.; Page, D. J. Y. S. *Polym. Eng. Sci.* **2004,** *44*, 1162.
25. Cerezo, F. T.; Preston, C. M. L.; Shanks R. A. *Macromol. Mater. Eng.* **2007,** *292*, 155.
26. Zipper, P.; Chernev, B.; Schnetzinger, K. *Macromol. Symp.* **2002,** *181*, 411.
27. Peng, S, W.; Wang, X. Y.; Dong, L. S. S. *Polym. Compos.* **2005,** *26*, 37.
28. Szabo, T.; Berkesi, O.; Forgo, P.; Josepovits, K.; Sanakis, Y.; Petridis, D.; Dekany, I. *Chem. Mater.* **2006,** *18*, 2740.
29. Du, X. S.; Xiao, M.; Meng, Y. Z.; Hay, A.S. *Carbon* **2005,** *43*, 195.
30. Sangeeta, H.; Neelima, B.; Pravin, K.; Rajendra, K.; Jog, J. P. *J. Polym. Sci. Part B: Polym. Phys.* **2001,** *39*, 446.
31. Zhao, Y. F.; Xiao, M.; Wang, S. J.; Ge, X. C.; Meng, Y. Z. *Compos. Sci. Technol.* **2007,** *67*, 2528.
32. Qu, B.; Xie, R. *Polym. Int.* **2003,** *52*, 1415.